

REGIONAL PROBLEMS OF EARTH'S CRYOLOGY

DOI: 10.21782/EC2541-9994-2018-5(3-16)

**WINTER AIR PALEOTEMPERATURES AT 30–12 KYR BP
IN THE LOWER KOLYMA RIVER, PLAKHINSKII YAR YEDOMA:
EVIDENCE FROM STABLE ISOTOPES****Yu.K. Vasil'chuk^{1,2}, A.C. Vasil'chuk¹**¹*Lomonosov Moscow State University, Faculties of Geography and Geology,
1, Leninskie Gory, Moscow, 119991, Russia; vasilch_geo@mail.ru*²*Tyumen State University, 6, Volodarskogo str., Tyumen, 625003, Russia*

A continuous 15–18 m long exposed permafrost sequence of the Plakhinskii Yar ice complex with ice wedges (Karetovo yedoma, left bank of the Stadukhin Channel, lower Kolyma River) have been studied in terms of structure, stable isotopes, radiocarbon ages, major ion chemistry, and pollen spectra. The obtained data allow quantitative estimates of Late Pleistocene permafrost and climate conditions in the area between 30 and 12 Kyr BP. The study confirms the previous inference that local winters at 30–28 Kyr BP were much colder than at present.

Ice wedge, Late Pleistocene, permafrost, yedoma, oxygen isotope, radiocarbon, pollen and spores, water chemistry, Plakhino site, northeastern Yakutia

INTRODUCTION

We report data on ice wedges in syngenetic permafrost (yedoma) exposed at the Plakhino site on the left bank of the Stadukhin Channel in the lower reaches of the Kolyma River. The ice wedges and their host frozen sediments have been studied in terms of structure, stable isotopes, radiocarbon ages, major ion chemistry, and pollen spectra, with implications for Late Pleistocene climate change in the area, between 30 and 12 Kyr BP.

The sampled outcrop is a flat block of ice-rich sediments, 20–22 m above sea level, between the Stadukhin Channel and the Khallerchinskaya Tundra. It differs from other similar lower Kolyma sections in its structure and location in a relict forest with particular vegetation and microclimate patterns. The forest provided wood for the construction of Stadukhin Ostrog (fortress), an exceptional monument of the Russian history and culture from the times of pioneers who first explored the Kolyma and northern Yakutia areas. The old Stadukhin community dating back to the middle 17th – middle 18th centuries [Zharnikov *et al.*, 2013] was discovered southwest of Chersky community on the left bank of the Kolyma River. The Plakhino Yar yedoma was studied previously by D.A. Gilichinsky, S.A. Zimov, N.N. Kudryavtseva, M.O. Leibman, D.V. Mikhalev, A.A. Sashov, and a team of Japanese scientists headed by professor M. Fukuda [Fukuda *et al.*, 1997; Mikhalev *et al.*, 2012].

**STRUCTURE AND COMPOSITION
OF PERMAFROST**

Ice-rich Late Pleistocene sediments containing ice wedges which notably differ from those in other ice complex (yedoma) sequences in the lower reaches of the Kolyma River (Duvanny Yar, Zelyony Mys, Ust'-Omolon, etc.) were sampled at the Plakhino site on the left side of the Stadukhin Channel (Fig. 1, *a*). The 14–18 m high outcrop exposes the Karetovo ice complex at 68°40'43.8" N, 160°17'6.6" E (Fig. 1, *b*).

The exposed sediments have ice contents up to 45 % and fine or coarse reticulate cryostructures. Almost the whole section, at least 15 m (Fig. 2, *a*), consists of thick texturally heavy or medium silt with plant detritus and fuzzy sand lenses. Unlike other such sections, the Plakhinskii Yar outcrop exposes two cycles of ice wedges spaced at 3–4 m, with their 1–1.5 m wide top surfaces at depths of 1.2–1.8 m below the ground surface in the upper layer (Fig. 2, *b*) and at 8.5 m in the lower one. The ice wedges of the upper cycle bear signatures of periodic growth: 0.5–0.6 m wide shoulders, more distinctly pronounced on one side, at depths about 6 and 9 m. The lower ice wedges have similar sizes (1.8 m wide and 4.5 m high) and are rooted below the river water table. The total vertical size of the ice wedge system exceeds 14 m. Ice is mostly columnar (Fig. 2, *c*) and gray in color.

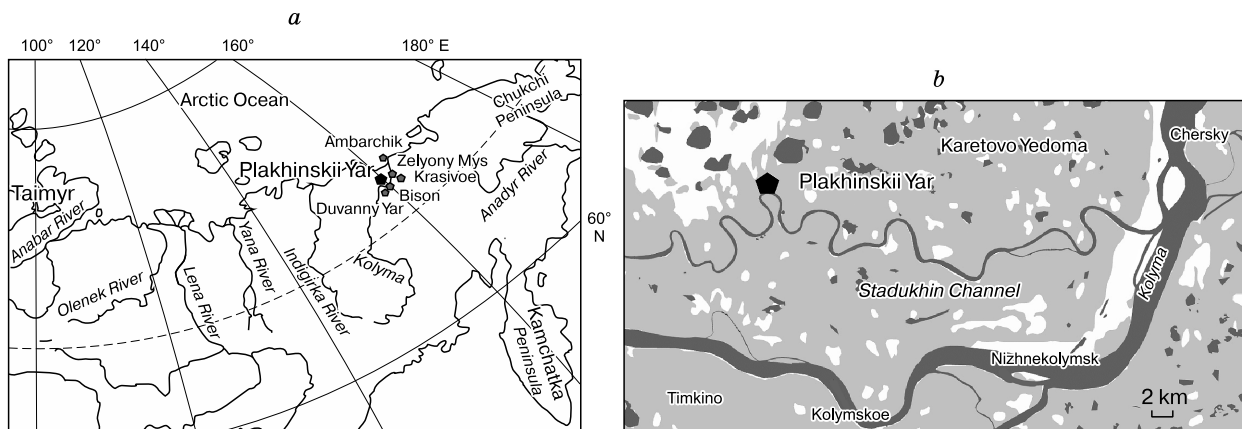


Fig. 1. Location maps of the Plakhinskii Yar in northeastern Yakutia (*a*) and in the left side of the Stadukhin Channel of the Kolyma River (the detailed map in panel *b* is based on *Google Map*).

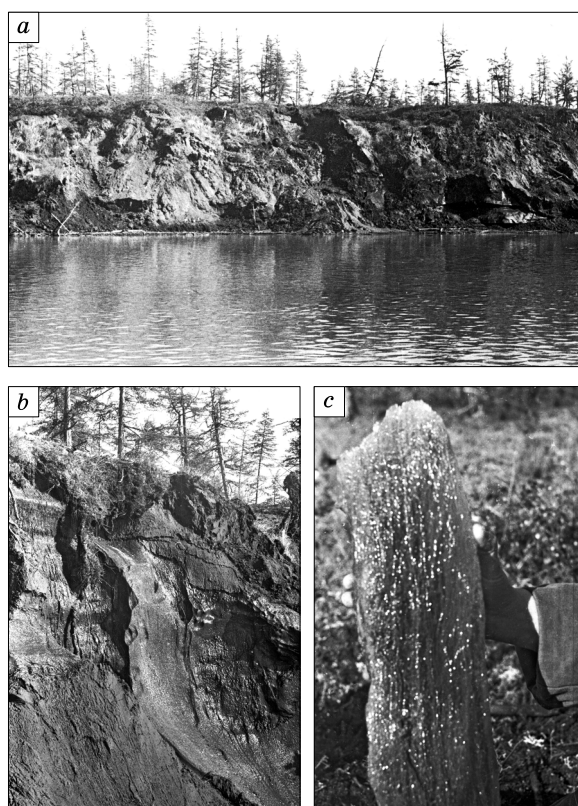


Fig. 2. Syngenetic Late Pleistocene ice wedges in the exposed Plakhinskii Yar ice complex (14–18 m terrace), Stadukhin Channel, Kolyma River. Photographs by Yu. Vasil'chuk.

a: general view; *b*: upper part of ice wedges; *c*: structure of Late Pleistocene ice wedges.

ANALYTICAL RESULTS

Radiocarbon dating of ice wedges and host sediments

Radiocarbon dating of plant detritus (mainly rootlets of grasses and twigs of subshrubs) found in permafrost was performed by the conventional beta counting method at the Geological Institute (Moscow), with participation of L.D. Sulerzhitsky. The dating has provided time constraints on the onset of deposition within the visible section part (30–27 Kyr), though the organic remnants are of limited amounts, concentrated mainly at the base of the section and disseminated in the middle (Table 1). The dates for the lower section part are reliable, judging by their consistency for samples treated in different ways in the field: one cleaned from silt and sand in the molten ice water before drying and two others dried without washing. Manually sampled rootlets from the section middle part, slightly below 6 m, have an age of 21.5 Kyr.

High-resolution ^{14}C AMS ages of particulate organic matter isolated from ice wedges were determined at the accelerator mass spectrometry facility of Seoul National University (SNU-AMS), by the team of J.C. Kim (Table 2). The obtained ages of SNU ice wedge samples are consistent and agree well with those for the host sediments: e.g., 21.4 and 21.5 Kyr for organic samples from ice and sediments, respectively, from depths of 8.6 m and 6 m (Table 1). The 21.5 Kyr BP age may mark the time when ice penetrated 2.0–2.5 m deep along frost cracks. Samples from depths of 4.5 m and 3.9 m in ice wedges gave 17.39 Kyr and 11.49 Kyr, respectively (Table 2).

The dating results were compared with the ^{14}C AMS ages of organic carbon (NUTA samples) from the Plakhinskii Yar Late Pleistocene syngenetic permafrost and ice wedges reported by Fukuda *et al.* [1997] (Table 3). The two datasets show good agree-

Table 1. Radiocarbon dates of organic remnants from Late Pleistocene syngenetic permafrost, Plakhinskii Yar*

Sample ID	Elevation asl, m	Depth, m	¹⁴ C-age, yr BP	Laboratory ID	Organic remnants
311-YuV/59	1.0	13	26 000 ± 1100	GIN-3980	Rootlets
311-YuV/60	1.5	12.5	27 000 ± 800	GIN-3981	Rootlets
311-YuV/71	1.0	13	31 500 ± 1100	GIN-3983	Rootlets with remnants of bugs and cones
NK-1**	8.0	6	21 500 ± 1100	GIN-4334	Rootlets

* 14–18-m terrace in the lower Kolyma River.

** Sampled by N. Kudryavtseva.

Table 2. Radiocarbon dates of particulate organic matter from Late Pleistocene ice wedges, Plakhinskii Yar*

Sample ID	Depth, m	¹⁴ C-age, yr BP	Laboratory ID	δ ¹³ C, organic, ‰
311-YuV/18	3.9	11 490 ± 80	SNU02-130	–30.4
311-YuV/6	3.9	13 130 ± 130	SNU02-129	–23.3
311-YuV/21	4.5	17 390 ± 200	SNU01-281	–40.4
311-YuV/29	8.6	21 400 ± 300	SNU02-131	–25.9

* 14–18-m terrace in the lower Kolyma River.

Table 3. Radiocarbon dates of organic remnants from Late Pleistocene syngenetic permafrost, Plakhinskii Yar*, according to [Fukuda et al., 1997]

Sample ID	Remnants	Depth, m	¹⁴ C age, yr BP	Laboratory ID	δ ¹³ C, organic, ‰
Sl-12	Twigs	3.32	20 680 ± 310	NUTA-4555	–28.00
Sl-11	Twigs	3.70	20 583 ± 982	NUTA-4273	–26.26
Sl-7	Twigs	5.51	22 280 ± 490	NUTA-4559	–24.39
Sl-2	Twigs	7.08	24 271 ± 973	NUTA-4272	–28.98
B-2	Rib of an even-hoofed mammal	8.57	29 300 ± 630	NUTA-4560	–20.37
S2-2	Twigs	9.38	27 290 ± 1110	NUTA-4558	–26.62

* 68°40'43.8" N, 160°17'6.6" E.

ment: the calibrated calendar ages of samples collected in different years fall within the same ranges (Figs. 3 and 4, a). Therefore, the yedoma deposits have been reliably dated and have a monotonic structure. The deposition most likely began about 32 Kyr BP.

Bearing in mind the principle that the youngest measured age of an ice sample is likely to be closest to its true age [Vasil'chuk and Vasil'chuk, 2017] and proceeding from the ages of organic matter disseminated in ice (Figs. 3 and 4, b), we infer that the exposed lower parts of the ice wedges began forming at 25–27 cal. Kyr BP, while the yedoma deposition lasted till 12 cal. Kyr BP. Thus, the obtained time constraints are quite reliable. The deposition rate was as fast as ~1.3 m per 1000 yr.

Major ion chemistry of ice and its host sediments

The contents of total dissolved solids (TDS) in ice and in the host permafrost were determined by titration at the Research Institute of Engineering for Construction (PNIIS, Moscow). Depth-dependent TDS contents in sediments show two prominent peaks (not solitary but in series) at depths of 12 m

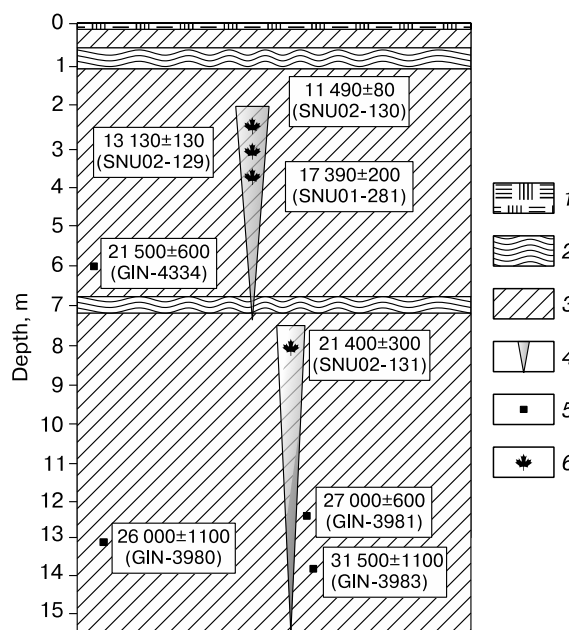


Fig. 3. Radiocarbon dates of permafrost and ice wedges.

1 – peat; 2 – sand; 3 – silt with rootlets and allochthonous peat; 4 – syngenetic ice wedges; 5, 6 – sampling sites for radiocarbon dating: yedoma deposits (5), ice wedges (6).

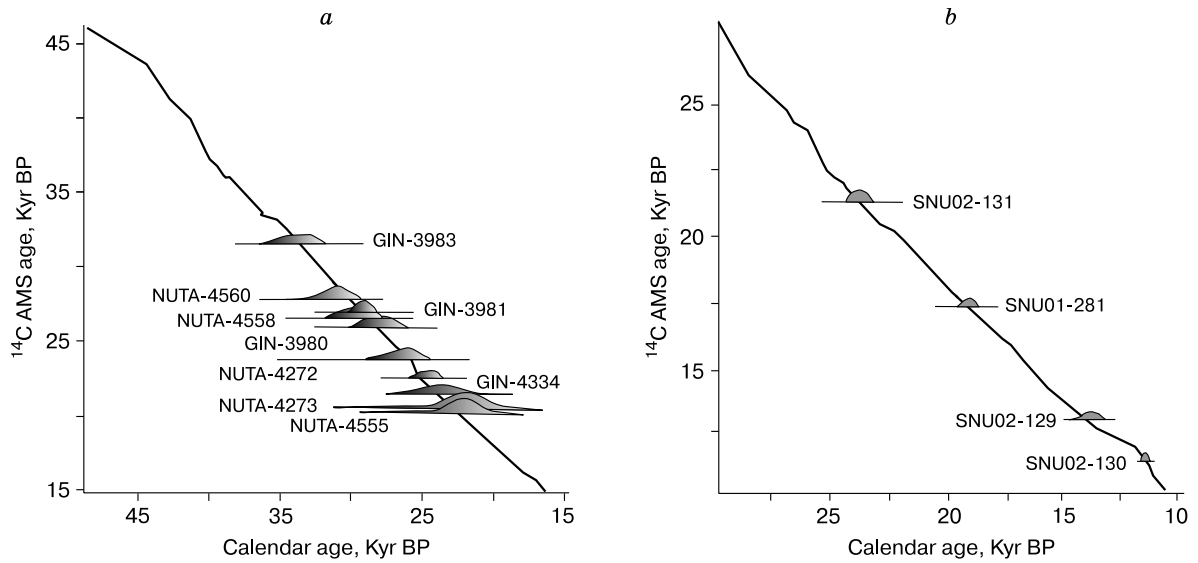


Fig. 4. ^{14}C AMS ages of permafrost (a) and ice wedges (b) at the Plakhinskii Yar site, obtained in different ways.

a: standard method on plant rootlets (GIN samples, Radiocarbon laboratory); accelerator mass spectrometry (NUTA samples, Tandetron AMS Facility, Nagoya, Japan); b: accelerator mass spectrometry of particulate organic carbon (SNU Samples, Accelerator Mass Spectrometry Facility, Seoul University, Korea). Ages are calibrated to calendar years before present (1950 AD).

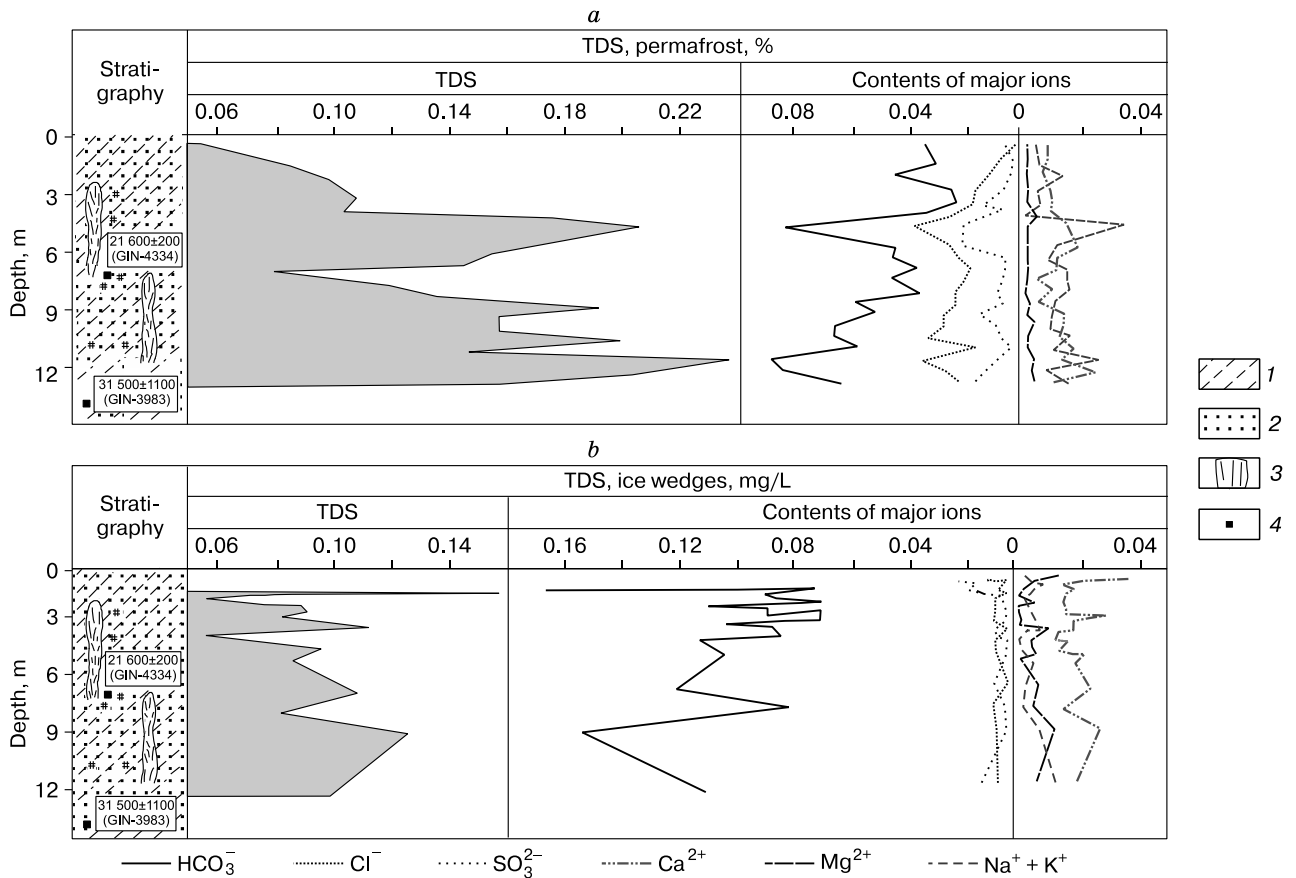


Fig. 5. Chemical diagrams of permafrost (a) and syngenetic ice wedges (b), Plakhinskii Yar site.

1 – silt with rootlets and allochthonous peat; 2 – sand; 3 – ice wedges; 4 – sampling sites for ^{14}C .

Table 4. Major ion chemistry: Late Pleistocene syngenetic permafrost, Plakhinskii Yar*

Sample ID	Depth, m	Total dissolved solids, %	Major ions, %						pH
			HCO ₃ ⁻	Cl ⁻	SO ₄ ²⁻	Ca ²⁺	Mg ²⁺	Na ⁺⁺ K ⁺	
311-YuV/46	0.7	0.057	0.033	0.004	0.004	0.007	0.003	0.003	7.43
311-YuV/47	1.4–1.5	0.082	0.030	0.008	0.004	0.007	0.002	0.003	7.22
311-YuV/49	2.05–2.15	0.097	0.045	0.012	0.004	0.007	0.002	0.014	7.28
311-YuV/50	3.1	0.108	0.025	0.014	0.007	0.010	0.004	0.007	7.10
311-YuV/51	3.8–3.9	0.101	0.023	0.015	0.014	0.010	0.003	0.006	7.66
311-YuV/52	3.9–4.0	0.172	0.031	0.024	0.007	0.009	0.008	0.002	7.54
311-YuV/53	4.9	0.208	0.082	0.040	0.022	0.017	0.005	0.036	7.81
311-YuV/54	6.3	0.155	0.043	0.022	0.021	0.019	0.003	0.012	7.48
311-YuV/55	6.7–6.8	0.143	0.043	0.017	0.006	0.013	0.003	0.010	7.54
311-YuV/56	7.0–7.1	0.078	0.036	0.016	0.005	0.013	0.003	0.014	7.45
311-YuV/57	7.8–7.9	0.118	0.045	0.019	0.006	0.006	0.004	0.014	7.30
311-YuV/58	8.5–8.6	0.135	0.036	0.023	0.009	0.011	0.003	0.017	6.94
311-YuV/61	9.2–9.3	0.192	0.061	0.022	0.006	0.008	0.006	0.011	7.77
311-YuV/62	9.4–9.5	0.157	0.051	0.028	0.014	0.018	0.004	0.015	7.13
311-YuV/63	10.0–10.1	0.157	0.065	0.025	0.009	0.017	0.005	0.015	7.02
311-YuV/64	10.5–10.6	0.206	0.064	0.032	0.005	0.015	0.003	0.017	7.82
311-YuV/65	11.0–11.1	0.146	0.056	0.016	0.003	0.021	0.004	0.011	7.88
311-YuV/66	11.3–11.4	0.236	0.084	0.036	0.008	0.018	0.005	0.029	7.20

* 14–18-m terrace in the lower Kolyma River.

and 4.5 m, where dry residue exceeds 0.2 % (Fig. 5, *a*; Table 4). Note also considerable contents of chloride ions, which are responsible for the greatest part of TDS peaks in the sediments, together with bicarbonate (HCO₃⁻). Sediments in the lower section part contain more chloride (Cl⁻) than sulfate (SO₄²⁻) ions (mmol/L), and their ratio decreases gradually upward from 6.4 to 1.0 (Fig. 6, *a*). The Cl⁻/SO₄²⁻ ratio varies in four cycles: from 6.40 to 4.5 at the depths 9.5–11.4 m; 2.0 to 3.67 at 9.4–6.5 m; 1.05 to 3.43 at 6.3–3.3 m; and 1.0 to 3.0 at 3.1–0.7. The ice

wedges show less distinct TDS cyclicity with smaller ranges of contents (Fig. 5, *b*; Table 5); the residue likewise decreases generally upward from 110–150 mg/L to 80–100 mg/L (though there is a peak of 188 mg/L in the upper section part). The predominance of HCO₃⁻ in ice is more prominent than in permafrost. Chloride ions are low, most often inferior to sulfates. The Cl⁻/SO₄²⁻ ratio varies periodically within 0.4–1.6 (Fig. 6, *b*) and indicates a mainly meteoric origin of the water that produced the ice wedges.

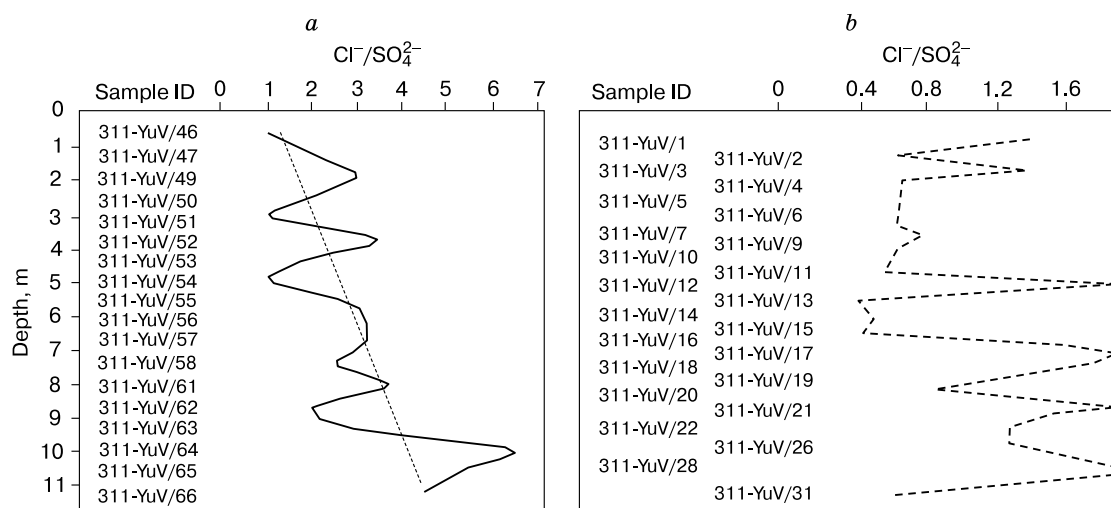
Fig. 6. Chloride/sulfate ratio in permafrost (*a*) and ice wedges (*b*), Plakhinskii Yar site.

Table 5. Major ion chemistry: ice wedges, Plakhinskii Yar*

Sample ID	Depth, m	Total dissolved solids, mg/L	Major ions, mmol/L						pH
			HCO ₃ ⁻	Cl ⁻	SO ₄ ²⁻	Ca ²⁺	Mg ²⁺	Na ⁺⁺ K ⁺	
311-YuV/1	1.8–2.0	86.0	1.20	0.18	0.12	0.75	0.50	0.18	6.83
311-YuV/2	1.5–1.6	188.0	2.65	0.24	0.43	1.99	1.22	0.14	7.22
311-YuV/3	1.8–2.0	98.0	1.35	0.20	0.14	0.88	0.42	0.26	6.81
311-YuV/4	1.8–2.0	106.0	1.15	0.22	0.34	0.73	0.42	0.35	13.8
311-YuV/5	1.8–2.0	104.0	1.45	0.16	0.26	0.95	0.64	0.20	6.92
311-YuV/6	1.8–2.0	90.0	1.10	0.16	0.26	0.83	0.47	0.16	6.95
311-YuV/7	1.8–2.0	116.0	1.57	0.22	0.28	1.13	0.63	0.21	7.15
311-YuV/9	2.15–2.30	98.0	1.43	0.16	0.22	1.00	0.61	0.15	7.15
311-YuV/10	2.15–2.30	108.0	1.40	0.14	0.29	0.97	0.50	0.24	7.12
311-YuV/11	2.15–2.30	90.0	1.12	0.12	0.19	0.78	0.46	0.14	6.83
311-YuV/12	2.15–2.30	82.0	1.12	0.21	0.10	0.71	0.38	0.22	6.64
311-YuV/13	2.15–2.30	108.0	1.76	0.08	0.22	1.21	0.67	0.15	7.15
311-YuV/14	2.70–2.90	114.0	1.43	0.18	0.28	0.97	0.59	0.22	7.10
311-YuV/15	2.70–2.90	114.0	1.55	0.14	0.26	1.12	0.61	0.16	7.06
311-YuV/16	2.70–2.90	102.0	1.33	0.24	0.14	0.99	0.38	0.22	7.26
311-YuV/17	2.70–2.90	128.0	2.04	0.19	0.09	1.61	0.41	0.22	7.09
311-YuV/18	3.9–4.1	140.0	1.68	0.25	0.14	0.71	1.19	0.14	6.95
311-YuV/19	3.9–4.1	106.0	1.37	0.16	0.17	0.80	0.69	0.16	6.59
311-YuV/20	3.9–4.1	88.0	1.33	0.20	0.09	0.88	0.50	0.16	7.28
311-YuV/21	5.0–5.2	116.0	1.69	0.20	0.12	1.04	0.63	0.24	7.22
311-YuV/22	5.0–5.2	126.0	1.83	0.18	0.14	1.12	0.78	0.19	7.39
311-YuV/26	7.1–7.2	138.0	1.99	0.22	0.17	1.40	0.72	0.20	7.43
311-YuV/28	8.1–8.2	102.0	1.27	0.21	0.10	0.70	0.69	0.14	6.98
311-YuV/31	9.4–9.5	156.0	2.44	0.21	0.10	1.54	0.95	0.21	6.86
311-YuV/39	12.2–12.3	128.0	1.74	0.20	0.26	1.16	0.61	0.29	7.44

* 14–18-m terrace in the lower Kolyma River.

Pollen records from ice wedges and permafrost

The Plakhinskii Yar pollen diagram is based on 46 samples: 30 samples of sediments and 16 samples of ice (Fig. 7). The percentages of components were calculated relative to the total contents of pollen and spores. The pollen spectra of the permafrost samples mainly contain local components and have monotonous depth-dependent patterns with predominant subshrub and herb pollen (73 to 96 %) and with poorly detectable deformed and immature pollen of dicotyledons. The spores mainly belong to *Selaginella sibirica* spikemoss, while those of sphagnum and green moss are few. Generally, tricolpate herb pollen predominates (52.8 to 91.0 %). However, the immature pollen cannot survive in unfavorable taphonomic conditions. Indeed, it is absent from modern samples but was found in new snow fallen in August in the vicinity of the Duvanny Yar section (12–23 %). The presence of immature pollen provides evidence of abrupt freezing and a short vegetation season insufficient for pollen maturation. In the case of the Plakhino pollen spectra, it was possibly a combination of the

vegetation period brevity and fast deposition. Thus, large amounts of pollen remained immature because the ground froze up while the plants were blooming and before the pollen degraded.

Moderate percentages of mechanically disturbed pollen grains and spores (8–15 %) correspond to deposition in a floodplain environment, while stable spore and pollen contents indicate quite high productivity of meadow communities in the respective time. The vegetation period was short but rather warm to maintain rapid growth of herbs and grasses and broad extent of meadows. The Plakhinskii Yar pollen diagram contains two peaks of immature tricolpate pollen, at depths 9.5–12.5 m (24–21 Kyr BP) and 4–6 m (~17–14 Kyr BP). They were the time spans when most of herb pollen could not mature while the sediments were deposited at high rates. On the other hand, the presence of larch pollen (4 grains at a depth of 6.3 m in sand and a few grains in ice wedges from the upper layer, at 8.1–9.4 m, Table 6) records favorable vegetation conditions. Therefore, larch trees grew within a short distance. Note also that each peak of immature pollen contents is preceded by a small peak of *Artemisia* sp. and *Pinus pumila*, while a local

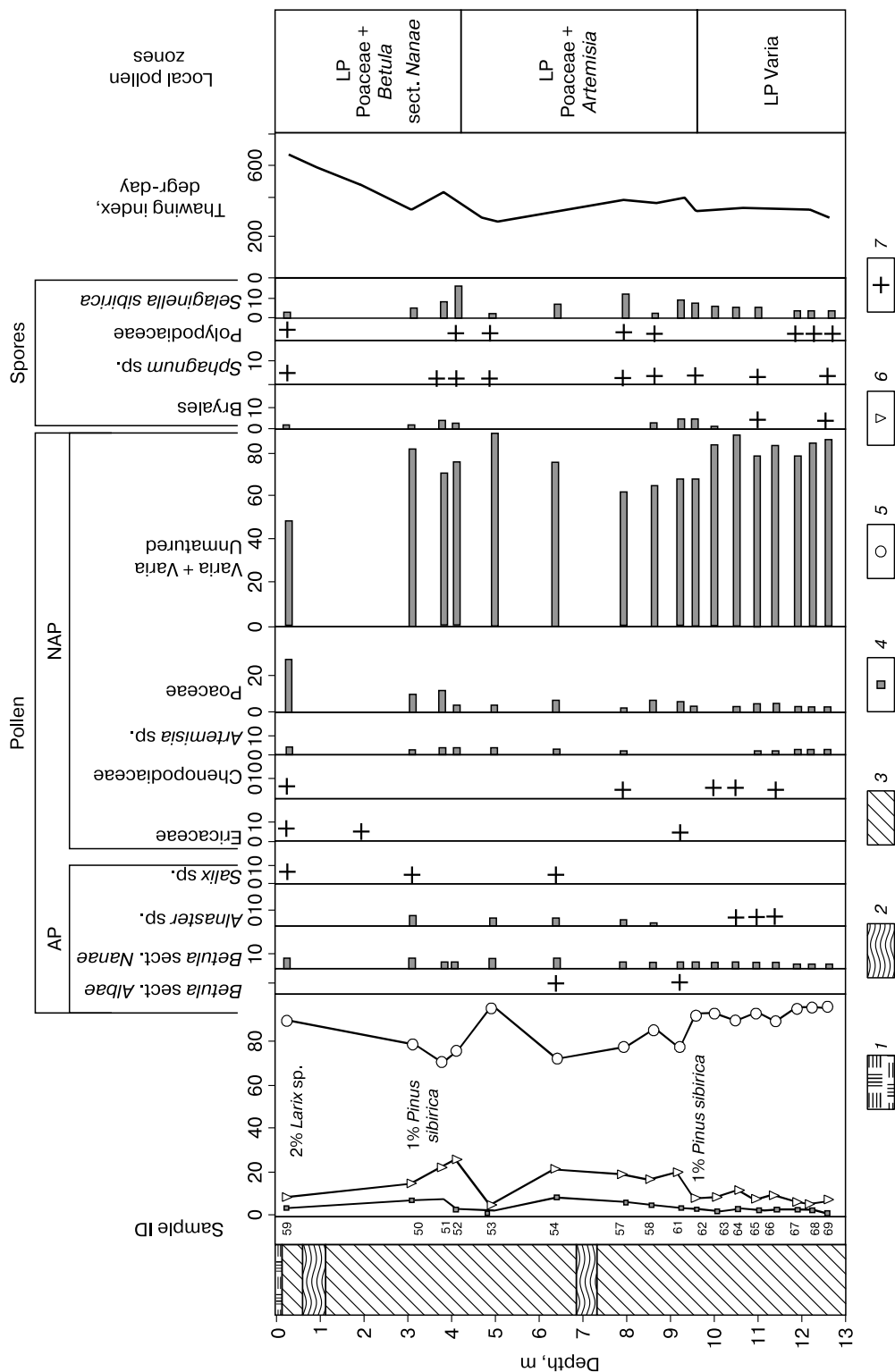


Fig. 7. Pollen diagram of Plakhinskii Yar yedoma.

1 – peat and plant remnants; 2 – silt; 3 – sand; 4 – silt with rootlets and allochthonous peat; 5 – percentages of shrub pollen (4), herb and subshrub pollen (5); spores (6); 7 – contents < 1 %.

Table 6. Spore and pollen percentages in samples dated from particulate organic matter in Late Pleistocene ice wedges, Plakhinskii Yar*

Ice wedges	Sample ID												
	311-YuV/13	311-YuV/18	311-YuV/20	311-YuV/21	311-YuV/22	311-YuV/26	311-YuV/28	311-YuV/29	311-YuV/31	311-YuV/39			
Depth, m	2.2	3.9	4.0	4.5	5.0	7.2	8.1	8.6	9.4	12.2			
AMS ¹⁴ C ages, particulate organic carbon		11 490 ± 80			17 390 ± 200			21 400 ± 300					
δ ¹⁸ O in ice, ‰	-29.9	-30.9		-33.6		-33.2	-32.6		-33.0	-33.0			
AP	-	-	-	-	-	-	4		2	-			
Tree pollen	9	25		9		15	8		13	2			
Shrub pollen	70	55		75		57	56		65	76			
NAP	21	20		16		28	32		20	22			
Spores	-	-	-	-	-	-	4		2	-			
<i>Larix</i>	-	-	-	-	-	-	-		-	-			
<i>Pinus sibirica</i>	-	-	-	-	-	-	-		-	-			
<i>Betula</i>	-	-	-	-	-	-	-		-	-			
<i>Betula</i> sect. <i>Nanae</i>	3	-	-	3		2	-		2	-			
<i>Alnaster</i>	3	-	-	3		-	-		2	-			
<i>Salix</i>	-	-	-	-		-	-		-	-			
Poaceae	8	-	-	10		3	4		15	36			
Ericaceae	3	-	-	5		-	-		-	4			
Chenopodiaceae	7	-	-	-		-	-		-	2			
<i>Artemisia</i>	25	20		23		9	16		21	6			
<i>Varia</i>	27	35		37		45	36		29	28			
<i>Bryales</i>	-	-	-	-		2	-		-	-			
<i>Sphagnum</i> sp.	-	-	-	3		2	-		-	-			
Polypodiaceae	3	-	-	-		-	-		-	-			
<i>Selaginella sibirica</i>	18	20		13		24	32		20	20			
Grains/L	144	80		156		220	100		166	224			
Reworked pollen	-	-	-	2		1	-		1	2			

Note. Italicized are samples dated by AMS.

* 14–18-m terrace in the lower Kolyma River.

peak of *Betula* sect. *Nanae* (6.3 %) coincides with the upper peak of immature pollen. Furthermore, the peaks of *Artemisia* correlate with those of TDS, which prompts correlation between climate humidity and pollen spectra.

The pollen spectra of ice wedges at the site (Table 6) record a regional-scale pollen rain. Since the contents of immature tricolpate pollen are much lower in ice than in sediments, this is obviously a local component associated with particular plant communities. The pollen of *Artemisia* and Poaceae have higher contents and are of regional extent. Peaks of *Artemisia* in these spectra can be interpreted as regional-scale predominance of xerophytic communities in the mosaic Arctic tundra. According to the obtained ^{14}C ages of ice, such plant communities may have been widespread during the 14–12 and 21–20 Kyr BP spans, which correlates with local peaks of *Artemisia* at depths of 10–11 m. *Larix* is present in 21–20 Kyr BP ice wedges and Chenopodiaceae are found in ice dated at 14–12 Kyr BP. These data, along with the presence of a Poaceae peak (36 %) at the base of an ice wedge, with an interpolated age of 23–22 Kyr BP, allow tracing pollen rain variations during the formation of ice wedges in the upper layer and in the upper part of the lower layer.

Vegetation conditions during the yedoma formation

The Plakhinskii Yar pollen spectra include three local zones (Fig. 7). Zone 1 (depths 14.0–9.5 m): predominant *Varia*, with a tentative age of 24–18 Kyr BP; no shrub pollen; high percentages of herb pollen, often immature; moderate amounts of *Angelica*, Asteraceae, Brassicaceae, Chichorioideae, Caryophyllaceae, *Epilobium*, *Galium*, *Koenigia*, *Oxyria*, *Polygonum aviculare*, Polygonaceae, Saxifragaceae, and *Senecio*; minor *Artemisia* and Poaceae. The conditions were possibly favorable for *Larix*, but its amount was limited: the found larch pollen is restricted to a few grains in the sand layer on the section periphery and in ice wedges, while macro remnants are absent from sediments. The percentage of *Selaginella sibirica* spores increases slightly upward, which indicates a humidity about the modern level. The pollen composition of grasses records the existence of vegetated ice wedge polygons in the Arctic tundra. The total of positive air temperatures (total annual thawing index) was likely 200–250 degr-day. Zone 2 (9.5–3.9 m): Poaceae + *Artemisia*, about 18–14 Kyr BP. Drier climatic conditions, judging by high percentages of *Artemisia* and Poaceae pollen. Very high percentages of immature grass pollen (89 %) correspond to very harsh vegetation conditions, while *Selaginella* peaks apparently record accelerated deposition. The reconstructed total annual thawing index values vary within 200–300 degr-day and correspond to the

Arctic tundra. Zone 3 (3.9–0.1 m): predominant Poaceae + *Betula* sect. *Nanae*, ~14–11 Kyr BP. High percentages of Poaceae and *Betula Nanae*, with moderate immature pollen (20–32 %), record a more favorable climate. Total annual thawing index values during the yedoma formation in the 3.9–0.1 m depth interval grew to 450–500 degr-day [Vasil'chuk, 2003].

Thus, the section displays abundant immature pollen of grasses and changes in subdominant taxa. The pollen spectra with *Artemisia* and *Betula* sect. *Nanae* give way to those with Poaceae at 9.5–12 and 4–6 m. However, the changes are smoothed out by high percentages of immature grass pollen.

Generally, the sediments were deposited in the conditions of short vegetation periods and abrupt transitions from positive to negative temperatures.

The pollen spectra of the dated ice wedge samples (Table 6) show ecologically consistent percentages of components and are free from pre-Quaternary palynomorphs. They contain thin-walled pollen grains of *Salix* and *Larix*, which cannot survive redeposition, as well as immature grains of tricolpate pollen identified as *Varia*. Therefore, the pollen spectra show the absence of reworked while the ^{14}C ages of particulate organic carbon are reliable to a high probability.

Stable isotopes in the Plakhinskii Yar ice wedges

The oxygen isotope composition of fifteen ice wedge samples ($\delta^{18}\text{O}$ values from -33.4 to -26.4 ‰ (Table 7); -27.0 to -26.4 ‰ for an offshoot of a syngenetic ice wedge) provides solid evidence for harsh climatic conditions during their formation. The most severe winters are recorded in very low $\delta^{18}\text{O}$ value of -34 ‰ in the lower part of the curve (Fig. 8) corresponding roughly to a time span of 30–28 Kyr BP, which is equated to Heinrich event 3 and appears also in the Plakhinskii Yar pollen spectra [Vasil'chuk, 2003]. The curve segment with ≥ -31.0 ‰ $\delta^{18}\text{O}$ (15–13 cal. Kyr BP) represents cryological conditions only slightly colder than the present climate, while most of the diagram shows $\delta^{18}\text{O}$ values at least -32.0 ‰ indicating winters much more severe than now. This result is consistent with $\delta^{18}\text{O}$ and $\delta^2\text{H}$ patterns in ice lenses from the same yedoma (Fig. 9).

Average oxygen and hydrogen isotope compositions of precipitation were studied near Chersky community. According to the Global Network of Isotopes in Precipitation (GNIP) records [<https://nucleus.iaea.org/wiser/index.aspx>] (Table 8), $\delta^{18}\text{O}$ and $\delta^2\text{H}$ values of snow vary considerably. By the end of winter, in March, $\delta^{18}\text{O}$ value -31.77 ‰ and $\delta^2\text{H}$ is -250.1 ‰. The respective values of rainfall in May, when meltwater penetrates into frost cracks, are on average -18.12 ‰ and -151.5 ‰.

Table 7. $\delta^{18}\text{O}$ variations in Late Pleistocene and Holocene ice wedges and in growing present ice wedges (PIW), Plakhinskii Yar*

Sample ID	Depth, m	$\delta^{18}\text{O}$, ‰	Ice type	Sample ID	Depth, m	$\delta^{18}\text{O}$, ‰	Ice type
<i>Late Pleistocene syngenetic ice wedges, Plakhinskii Yar</i>							
311-YuV/1	1.8	-33.1	Ice wedge	311-YuV/28	8.1	-32.6	Ice wedge
311-YuV/3	1.9	-30.9	Ice wedge	311-YuV/29	8.6	-32.1	Ice wedge
311-YuV/6	2.0	-30.8	Ice wedge	311-YuV/31	9.4	-33.0	Ice wedge
311-YuV/12	2.2	-31.0	Ice wedge	311-YuV/33	10.2	-33.7	Ice wedge
311-YuV/13	2.7	-29.9	Ice wedge	311-YuV/35	11.0	-32.8	Ice wedge
311-YuV/16	4.0	-30.9	Ice wedge	311-YuV/37	11.7	-33.6	Ice wedge
311-YuV/21	5.0	-33.6	Ice wedge	311-YuV/39	12.2	-33.0	Ice wedge
311-YuV/24	6.3	-33.4	Ice wedge	311-YuV/41	13.2	-32.9	Ice wedge
311-YuV/26	7.1	-33.2	Ice wedge	311-YuV/44	14.5	-34.7	Ice wedge
311-YuV/25	7.2	-32.1	Ice wedge				
<i>Late Pleistocene syngenetic ice wedges, alas deposits exposed near Plakhinskii Yar outcrop</i>							
312-YuV/4	1.7	-26.5	Ice wedge	312-YuV/6	1.7	-27.4	Ice wedge
312-YuV/5	1.1	-27.1	Ice wedge	312-YuV/7	3.1	-27.2	Ice wedge
<i>Present ice wedges growing into ice wedges from alas deposits</i>							
312-YuV/1	0.1	-27.0	PIW	312-YuV/12	0.35	-25.3	PIW
312-YuV/2	0.5	-27.1	PIW	312-YuV/13	0.65	-23.4	PIW
312-YuV/3	0.5	-26.4	PIW				

* 14–18-m terrace in the lower Kolyma River.

Monthly mean $\delta^{18}\text{O}$ and $\delta^2\text{H}$ values in falling snow at the Chersky site are from -36.7 to -22 ‰ and -279.2 to -169.4 ‰, respectively [Konyakhin *et al.*, 1996]. However, meltwater may penetrate into frost cracks from late spring snow with average $\delta^{18}\text{O} = -27.6$ ‰, which is close to the values in offshoots of modern ice wedges that are forming in the Kolyma lower reaches near Chersky community (-24 to -26 ‰).

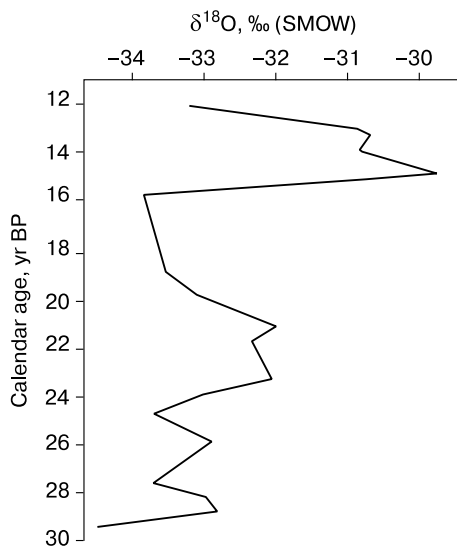


Fig. 8. $\delta^{18}\text{O}$ variations in Late Pleistocene ice wedges (Plakhinskii Yar site) as a function of calibrated ^{14}C ages of ice wedges.

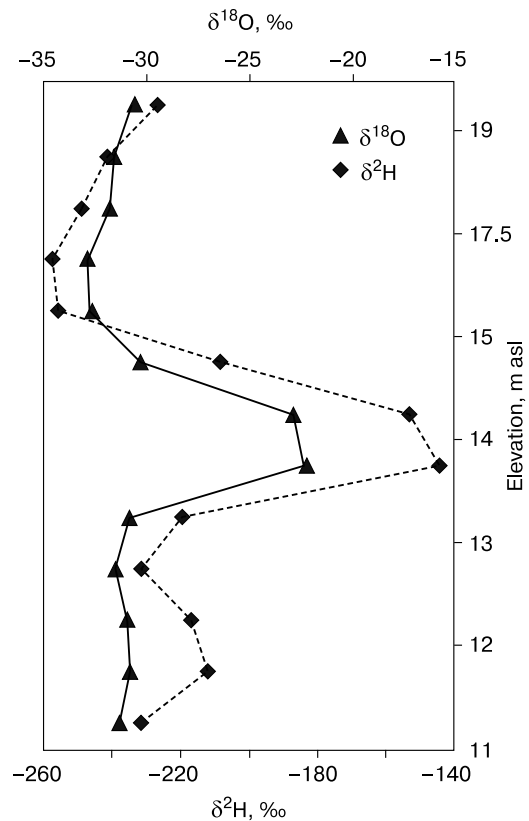


Fig. 9. Depth-dependent variations of $\delta^{18}\text{O}$ and $\delta^2\text{H}$ in ice wedges, Plakhinskii Yar site, after [Mikhalev *et al.*, 2012].

Table 8. Variations of mean monthly $\delta^{18}\text{O}$, $\delta^2\text{H}$ and d_{exc} in precipitation near Chersky for 2001–2010

Month	$\delta^{18}\text{O}$, ‰	$\delta^2\text{H}$, ‰	d_{exc} , ‰
January	-34.61 ± 3.93	-265.0 ± 28.3	11.9 ± 3.4
February	-32.10 ± 2.62	-247.3 ± 22.2	9.5 ± 1.3
March	-31.77 ± 3.62	-250.1 ± 28.7	4.0 ± 5.3
April	-25.58 ± 4.22	-215.3 ± 32.5	4.9 ± 3.8
May	-18.12 ± 3.44	-151.5 ± 23.2	-1.0 ± 9.8
June	-18.34 ± 4.29	-156.5 ± 42.0	2.0 ± 2.8
July	-17.90 ± 2.51	-142.7 ± 5.5	3.4 ± 2.7
August	-17.32 ± 1.65	-135.6 ± 12.5	3.7 ± 2.1
September	-17.54 ± 2.02	-135.0 ± 13.4	6.7 ± 2.4
October	-23.77 ± 3.45	-178.5 ± 24.2	11.7 ± 6.9
November	-27.28 ± 3.45	-204.4 ± 20.7	13.9 ± 8.0
December	-30.90 ± 3.94	-233.4 ± 31.8	13.8 ± 5.3

Note. Data from GNIP database (<https://nucleus.iaea.org/wiser/index.aspx> [Partner: Northeast Science Station, Cherskij]).

$\delta^{18}\text{O}$ VARIATIONS IN OTHER YEDOMAS FROM THE LOWER KOLYMA AREA COEVAL TO THE PLOKHINSKII YAR ICE COMPLEX

The oxygen isotope composition of ice wedges at the Plakhino site is remarkable by extremely light $\delta^{18}\text{O}$, especially at the wedge bottom (Fig. 8, 10, a), which records very cold winters in the Late Pleistocene. Thus, $\delta^{18}\text{O}$ in the Plakhinskii Yar ice wedges is markedly lower than in similar coeval ice wedges elsewhere in northeastern Russia [Vasil'chuk and Vasil'chuk, 1998, 2014, 2017]. This result confirms the inference of a harsh geocryological setting based on close spacing of ice wedges.

Some parts of the Plakhinskii Yar yedoma were deposited synchronously with other yedoma sequences in the Kolyma lower reaches: Krasivoe outcrop in the right side of the Mal'yi Anyui River; Aleshkinskaya terrace; Bison outcrop in the mouth of the Lakeevskaya Channel; Duvanny Yar and Zelyony Mys (yedoma upper parts); vicinities of Ambarchik community, Kolyma mouth.

Permafrost near *Ambarchik community* ($69^{\circ}39' \text{N}$, $162^{\circ}18' \text{E}$) contains large amounts of redeposited organic matter, judging by inversion of ^{14}C dates, as estimated by M. Fukuda, A. Sashov, and their team [Fukuda et al., 1997]. We may hypothesize that the upper one third of the section was deposited soon after 32 Kyr BP; ice wedges have -32.6 ‰ $\delta^{18}\text{O}$ values on average (Fig. 10, b).

The *Krasivoe* outcrop ($68^{\circ}18'34'' \text{N}$, $161^{\circ}44'09'' \text{E}$) located in the right side of the Mal'yi Anyui River, 15 km upstream of Anyuisk community, exposes a low (15–17 m) depositional terrace. The section begins with horizontally laminated bluish-gray silt, 4–6 m of visible thickness. Sediments in the lower section part have ^{14}C ages from 18.7 to 27.3 Kyr

BP: $18\,700 \pm 1400$ yr BP (MGU-881), $22\,700 \pm 1500$ yr BP (MGU-886), and $27\,300 \pm 300$ yr BP (GIN-3209) [Sher and Plakht, 1988]. The $\delta^{18}\text{O}$ values are from -22.6 to -22.9 ‰ in ice wedges of the second generation, which all lie inside the silt unit, and from -30.5 to -32.0 ‰ in the crosscutting wedges of the first generation [Nikolaev et al., 2010; Mikhal'ev et al., 2012]. These values are consistent with previous estimates of -28.9 to -32.6 ‰ $\delta^{18}\text{O}$ [Konyakhin et al., 1996] and represent a colder climate than that for ice wedges up the section.

Samples of ice wedges from the Krasivoe site provide convincing evidence that the 30–28 Kyr BP time span was slightly colder than that of 24–22 Kyr BP (Fig. 10, c): -34.0 ‰ against -33.3 ‰ $\delta^{18}\text{O}$, on average [Fukuda et al., 1997].

Poor exposure of the *Aleshkinskaya terrace* ($68^{\circ}43' \text{N}$, $158^{\circ}42' \text{E}$) did not allow us to sample Late Pleistocene ice wedges: we found only thick Holocene wedges during our trip. However, there is published evidence from the Aleshkinskaya yedoma [Konyakhin et al., 1996], where latest Pleistocene ice wedges were sampled in the Krasivoe outcrop on the right bank of the Mal'yi Anyui and at Aleshkinskaya hunting lodge, in outcrops of commensurate heights (15–17 and 14–16 m, respectively). Samples from the Aleshkinskaya terrace (scarce plant remnants from sand in all cases) gave the ages $14,780 \pm 300$ yr BP at a depth of 5 m (SOAN-2307) and $17,260 \pm 140$ yr BP at 7 m (SOAN-2308) [Tomirdiario and Chernenkiy, 1987]. The previous dates were in a range of 15 to 16 Kyr BP [Chernenkiy and Fedorova, 1982]. The pollen spectra of the Aleshkinskaya terrace samples correlate well with those from the Plakhinskii Yar site [Chernenkiy and Fedorova, 1982], which suggests deposition during the same time spans.

We also dated the *Bison* yedoma exposure ($68^{\circ}33' \text{N}$, $159^{\circ}41' \text{E}$) from the right side of the Kolyma River, in the mouth of the Lakeevskaya Channel, 15 km downstream of the Duvanny rapids. ^{14}C AMS dating of particulate organic matter and pollen concentrate showed that ice wedges formed continuously from 32 to 26 Kyr BP. They have $\delta^{18}\text{O}$ from -33.32 to -32.02 ‰ (-33 ‰ on average), which indicates a mean January temperature of -50 °C, or 15 degrees colder than at present (-35 °C).

The ice wedges in the upper parts of the Krasivoe and Aleshkinskaya sections sampled by Konyakhin et al. [1996] most likely formed between 17 and 14–12 Kyr BP. Their $\delta^{18}\text{O}$ values are within -32.6 ‰, most often -29 to -31 ‰, contrary to the expectation that they would be more negative than in older layers corresponding to harsh climate conditions of that time. Therefore, the latest Late Pleistocene glaciation in the northern Kolyma plain (Sartan, MIS 2), although being cold, did not reach the minimum $\delta^{18}\text{O}$ and air temperature values of the preceding Karga

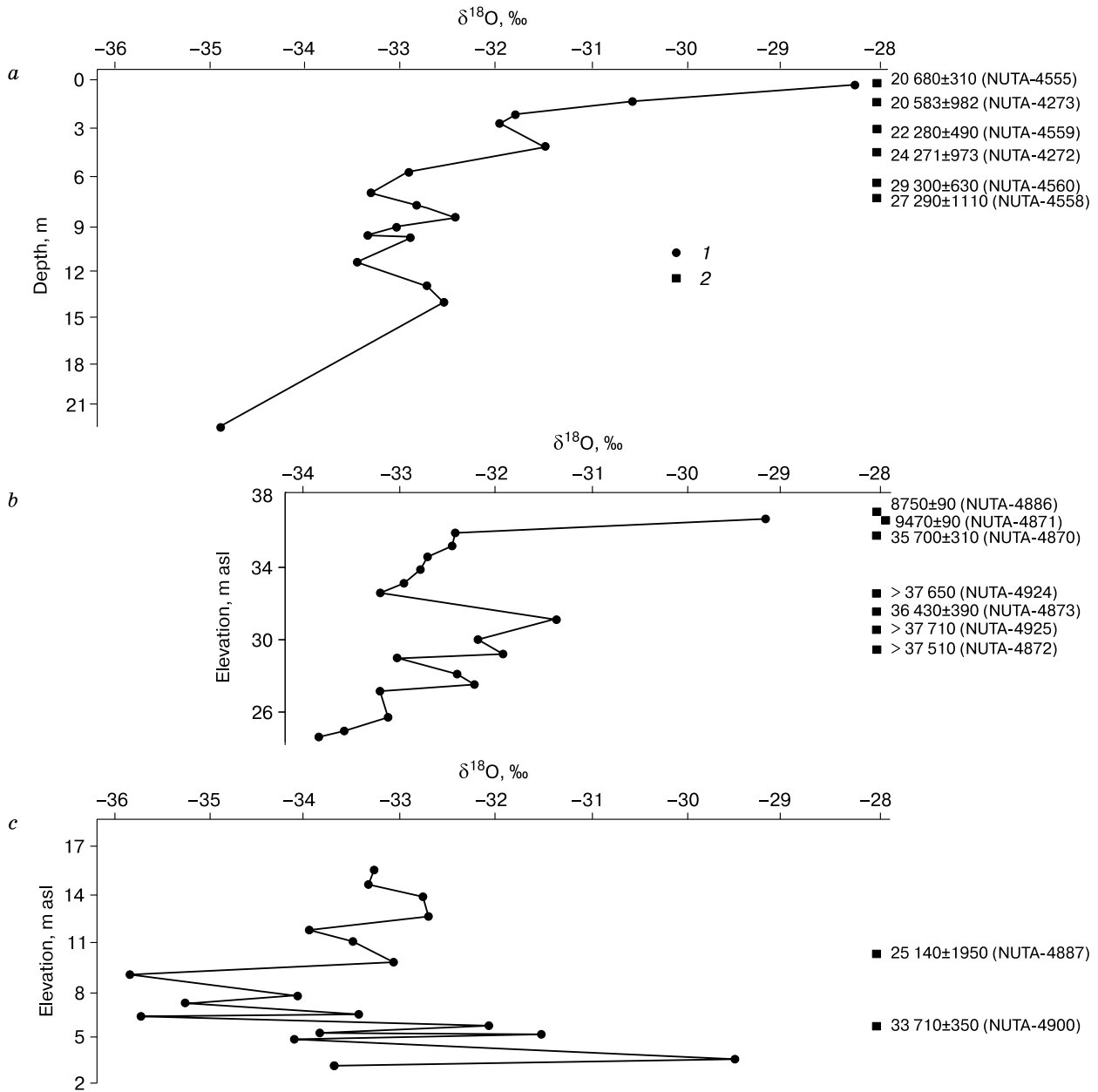


Fig. 10. $\delta^{18}\text{O}$ diagram and ^{14}C AMS ages of Late Pleistocene ice wedges in permafrost at different sites.

a: Plakhinskii Yar, Stadukhin Channel, Kolyma River; b: Ambarchik, Kolyma mouth; c: Krasivoe, Malyy Anyui River; 1 – $\delta^{18}\text{O}$ in ice wedges; 2 – sampling sites for dating, Nagoya University (NUTA samples, Tandetron AMS Facility) [Fukuda et al., 1997].

event (equated to MIS 3). As inferred by *Streletskaia et al.* [2015] based on published $\delta^{18}\text{O}$ data for ice wedges, the climate of the area was colder during MIS 3 than during the Sartan glacial (MIS 2).

Studies of eight Late Pleistocene (26 to 12.9 cal. Kyr BP) ice wedges and seven ice lenses stripped in the CRREL Permafrost Tunnel in Fox (Alaska) [Lachniet et al., 2012; Sloat, 2014] revealed a generally cold climate with one warmer and four colder events. The 26 to 12.9 Kyr BP time span cor-

responds to rapid formation of the Plakhino yedoma, as well as those exposed at the Krasivoe and Aleshkinskaya sites. The $\delta^{18}\text{O}$ values of the Fox permafrost tunnel samples [Sloat, 2014] are the most negative (-28.9 ‰) in Pleistocene ice wedges but are less depleted in modern snow (-22.3 ‰) and in young ice wedges (-21.8 ‰). Very low $\delta^{18}\text{O}$ indicate that ice wedges formed in a climate much colder than the present conditions [Lachniet et al., 2012; Sloat, 2014].

Table 9. Mean January air paleotemperatures (t_j°) and present values, compared, at different sites in lower Kolyma area. Modified after [Vasil'chuk, 1991, 2016]

Site	Parameter	Period (cal. yr BP)				Present	Reference
		30–28	24–22	20–18	16–12		
Plakhinskii Yar	$\delta^{18}\text{O}_{\text{PIW}}, \text{‰}$	-34.8	-31.6	-32.0	-31.1	-25.8	[Vasil'chuk, 1992; Fukuda et al., 1997]
	t_j°	-51.0	-47.0	-48.0	-46.0	-35.0	
Ambarchik	$\delta^{18}\text{O}_{\text{PIW}}, \text{‰}$	-32.6	–	–	–	-24.0	[Fukuda et al., 1997]
	t_j°	-49.0	–	–	–	-32.0	
Zelyony Mys	$\delta^{18}\text{O}_{\text{PIW}}, \text{‰}$	-31.6	-30.4	-31.6	-30.7	-25.5	[Vasil'chuk, 1992]
	t_j°	-47.0	-45.0	-47.0	-45.0	-33.0	
Duvanny Yar	$\delta^{18}\text{O}_{\text{PIW}}, \text{‰}$	-31.8	-32.2	-30.5	-31.0	-25.1	[Vasil'chuk, 1992, 2016]
	t_j°	-47.0	-48.0	-46.0	-46.0	-35.0	
Bison	$\delta^{18}\text{O}_{\text{PIW}}, \text{‰}$	-33.0	–	–	–	-26.0	[Vasil'chuk et al., 2001]
	t_j°	-50.0	–	–	–	-35.0	
Krasivoe	$\delta^{18}\text{O}_{\text{PIW}}, \text{‰}$	-34.0	-33.3	-31.0	–	-26.0	[Konyakhin et al., 1996; Fukuda et al., 1997; Nikolaev et al., 2010]
	t_j°	-51.0	-47.0	-46.0	–	-35.0	
Aleshkinskaya terrace	$\delta^{18}\text{O}_{\text{PIW}}, \text{‰}$	–	–	-31.0	–	-26.0	[Konyakhin et al., 1996]
	t_j°	–	–	-46.0	–	-35.0	

The coldest event in northern Alaska lasted from 27 to 21 cal. Kyr BP, the time of Itkillik II glaciation advance in the Brooks Range. According to reconstructions with reference to data on chironomids, summer climates (mean July air temperatures) at that time were on average 3.5 °C below the present temperatures around Burial Lake (335 km southwest of Itkillik) [Kurek et al., 2009] and 2.3 °C colder than the modern values in the area of Zagoskin Lake (from 25 to 17 cal. Kyr BP) [Kanetskiy et al., 2011; Lapointe et al., 2017]. As estimated by Lachniet et al. [2012, 2016] from $\delta^{18}\text{O}$ (–27.9 ‰) for ice wedges near Fairbanks, the mean winter temperature during the 26–22 cal. Kyr span in Alaska was –38 °C, or 17 °C colder than the respective present value (–21.1 °C).

On the other hand, Meyer et al. [2017] concluded that summers in the area of Kamchatka at 20–18 Kyr BP were as warm as now, proceeding from a paleothermometer based on biomarkers from clastic shelf sediments. The warm summer air temperatures may be due to a strong southern wind (stronger than now) above Kamchatka and an anticyclone above the Subarctic Pacific region. Therefore, climatic conditions in the geographically proximal areas of Alaska and Kamchatka have been different due to the influence of the Pacific ocean, which is an important climate agent. In this respect, special caution is required in paleotemperature correlations between the two areas.

WINTER AIR PALEOTEMPERATURES CONVERTED FROM $\delta^{18}\text{O}$ DATA

Mean winter ($t_{\text{wint.mean}}$) and January (t_j) air paleotemperatures for the lower Kolyma River were estimated with reference to empirical relationships between $\delta^{18}\text{O}$ values of present growing ice wedges ($\delta^{18}\text{O}_{\text{PIW}}$) and winter temperatures in the period of

their growth for the past 60–100 yr [Vasil'chuk, 1991, 1992]: $t_j = 1.5 \delta^{18}\text{O}_{\text{PIW}} (\pm 3 \text{ }^\circ\text{C})$, $t_{\text{wint.mean}} = \delta^{18}\text{O}_{\text{PIW}} (\pm 2 \text{ }^\circ\text{C})$. The two equations were used to calculate Late Pleistocene (30–12 Kyr BP) winter air temperatures for several reference sections in the lower Kolyma area (Table 9) [Vasil'chuk and Vasil'chuk, 2014].

According to the obtained radiocarbon ages and oxygen isotope compositions of ice wedges, winters were the coldest in the 30–28 Kyr BP time span when the mean January air temperature in the Kolyma valley fell to –47 °C or even –51 °C (Table 9), while the present range is –33 to –35 °C.

The period of cold winters (30–28 Kyr BP) is equated to Late Pleistocene Heinrich event 3 in the global climate chronology [Rasmussen et al., 2014]. The positive degree-day sums were also the smallest and the vegetation season was short during that time span.

CONCLUSIONS

The Plakhinskii Yar outcrop in the lower reaches of the Kolyma River exposes two-stage Late Pleistocene ice wedges with polygon sizes no more than 3–5 m.

The yedoma formation lasted from 32 to 12 cal. Kyr BP, while the exposed lower part of ice wedges began forming at 30–25 cal. Kyr BP.

Proceeding from the strongly negative oxygen isotope composition of ice wedges in the reference permafrost sections from the lower Kolyma, the whole 30–12 Kyr BP time span can be assigned to a single Late Pleistocene cryochron.

The climate in the end of that cryochron was colder than the modern climate, with notably harsher winters, as estimated from $\delta^{18}\text{O}$ of ice wedges at the Plakhinskii Yar, Zelyony Mys, Duvanny Yar, Krasivoe, and Ambarchik sites.

The lowest mean January air paleotemperatures in the area were 14–17 °C below the present values during the 30 to 28 Kyr BP period equated to Heinrich event 3 of the global climate history.

The paper profited much from thoughtful constructive criticism and valuable advice of the late Professor S.M. Fotiev.

The study was supported by the Russian Science Foundation (grant No. 14-27-00083-P) and by government funding to Moscow University. The mass spectrometry equipment was purchased for money allocated to the Development Program of Moscow University.

References

- Chernenkiy, B.I., Fedorova, I.N., 1982. Some structure and composition features of the Aleshkinskaya terrace deposits in the Kolyma River valley, in: Quaternary Deposits in the Eastern USSR. Northeastern Complex NII, Magadan, Issue 2, pp. 11–13 (Preprint)
- Fukuda, M., Nagaoka, D., Saijyo, K., Nakamura, T., Kunitsky, V., 1997. Radiocarbon dating results of organic materials obtained from Siberian permafrost areas. Rep. Inst. Low Temperature Sci., Hokkaido University, Sapporo, pp. 17–28.
- Kanevskiy, M., Shur, Y., Fortier, D., Jorgenson, M.T., 2011. Cryostratigraphy of late Pleistocene syngenetic permafrost (Yedoma) in northern Alaska, Itkillik River exposure. Quatern. Res. 75 (3), 584–596, DOI: 10.1016/j.yqres.2010.12.003.
- Konyakhin, M.A., Mikhalev, D.V., Konyakhin, M.A., Solomatina, V.I., 1996. Oxygen Isotope Composition of Ground Ice. Moscow University Press, Moscow, 156 pp. (in Russian)
- Kurek, J., Cwynar, L.C., Ager, T.A., Abbot, M.B., Edwards, M.E., 2009. Late Quaternary paleoclimate of western Alaska inferred from fossil chironomids and its relation to vegetation histories. Quatern. Sci. Rev. 28 (9–10), 799–811, DOI: 10.1016/j.quascirev.2008.12.001.
- Lachniet, M.S., Lawson, D.E., Sloat, A.R., 2012. Revised ¹⁴C dating of ice wedge growth in interior Alaska (USA) to MIS 2 reveals cold paleoclimate and carbon recycling in ancient permafrost terrain. Quatern. Res. 78, 217–225.
- Lachniet, M.S., Lawson, D.E., Stephen, H., Sloat, A.R., Patterson, W.P., 2016. Isoscapes of ^δ18O and ^δ2H reveal climatic forcings on Alaska and Yukon precipitation. Water Resources Res. 52 (8), 6575–6586, DOI: 10.1002/2016WR019436.
- Lapointe, E.L., Talbot, J., Fortier, D., Fréchet, B., Strauss, J., Kanevskiy, M., Shur, Yu., 2017. Middle to late Wisconsinan climate and ecological changes in northern Alaska: Evidence from the Itkillik River Yedoma. Palaeogeography, Palaeoclimatology, Palaeoecology, DOI: 10.1016/j.palaeo.2017.08.006.
- Meyer, V.D., Hefter, J., Lohmann, G., Max, L., Tiedeman, R., Mollenhauer, G., 2017. Summer temperature evolution on the Kamchatka Peninsula, Russian Far East, during the past 20 000 years. Climate of the Past 13, 359–377, DOI: 10.5194/cp-13-359-2017.
- Mikhalev, D.V., Nikolaev, V.I., Romanenko, F.A., 2012. Reconstruction of the Late Pleistocene–Holocene formation conditions of ground ice in the Kolyma Lowland. Bull. MGU, Ser. 5, Geografiya, No. 5, 35–42.
- Nikolaev, V.I., Mikhalev, D.V., Romanenko, F.A., Brill, M., 2010. Reconstruction of the formation conditions for permafrost in Northeastern Russia from isotope data (example from reference sections in the lower Kolyma Lowland). Led i Sneg 50 (4), 79–90.
- Rasmussen, S.O., Bigler, M., Blockley, S.P., Blunier, T., Buchardt, S.L., Clausen, H.B., Cvijanovic, I., Dahl-Jensen, D., Johnsen, S.J., Fischer, H., Gkinis, V., Guillevic, M., Hoek, W.Z., Lowe, J.J., Pedro, J.B., Popp, T.J., Seierstad, I.K., Steffensen, J.P., Svensson, A., Vallelonga, P.T., Vinther, B.M., Walker, M.J., Wheatley, J.J., Winstrup, M., 2014. A stratigraphic framework for abrupt climatic changes during the Last Glacial period based on three synchronized Greenland ice-core records: refining and extending the INTIMATE event stratigraphy. Quatern. Sci. Rev. 106, 14–28.
- Sher, A.V., Plakht, I.R., 1988. Radiocarbon dating and Pleistocene stratigraphy of lowlands in the northeastern USSR. Izv. AN SSSR, Ser. Geol., No. 8, 17–31.
- Sloat, A., 2014. Modern to Late Pleistocene Stable Isotope Climatology of Alaska. PhD Thesis UNLV Pap. 2143. Depart. Geosci. Univ. Nevada, Las Vegas, USA, 181 pp.
- Streletskaia, I.D., Vasiliev, A.A., Oblogov, G.E., Tokarev, I.V., 2015. Reconstruction of paleoclimate of Russian Arctic in Late Pleistocene–Holocene on the basis of isotope study of ice wedges. Earth's Cryosphere (Kriosfera Zemli) XIX (2), 86–94.
- Tomirdiaro, S.V., Chernenkiy, B.I., 1987. Cryogenic-Aeolian Deposits in the Eastern Arctic and Subarctic Areas. Nauka, Moscow, 198 pp. (in Russian)
- Vasil'chuk, A.C., 2003. Appearance of Heinrich events in radiocarbon dated pollen diagrams of ice wedges and its surrounding yedoma sediments of the lower Kolyma River. Kriosfera Zemli VII (4), 3–13.
- Vasil'chuk, Yu.K., 1991. Reconstruction of the palaeoclimate of the Late Pleistocene and Holocene of the basis of isotope studies of subsurface ice and waters of the permafrost zone. Water Resources 17 (6), 640–647.
- Vasil'chuk, Yu.K., 1992. Oxygen Isotope Composition of Ground Ice (Application to Paleogeocryological Reconstructions), Theor. Probl. Dept., RAS, Moscow University, Research Institute of Engineering for Construction (PNIIS), Moscow, Book 1, 420 pp, Book 2, 264 pp. (in Russian)
- Vasil'chuk, Yu.K., 2016. Spatio-temporal distribution of mean January air temperature over the Russian Arctic during 30–12 ka BP with high temporal resolution. Arktika i Antarktika (Arctic and Antarctic), No. 1, 86–103, DOI: 10.7256/2453-8922.2016.1.21310.
- Vasil'chuk, Yu.K., Vasil'chuk, A.C., 1998. Oxygen-isotope and ¹⁴C data associated with Late Pleistocene syngenetic ice-wedges in mountains of Magadan region, Siberia. Permafrost and Periglacial Processes 9 (2), 177–183.
- Vasil'chuk, Yu., Vasil'chuk, A., 2014. Spatial distribution of mean winter air temperatures in Siberian permafrost at 20–18 ka BP using oxygen isotope data. Boreas 43 (3), 678–687.
- Vasil'chuk, Yu.K., Vasil'chuk, A.C., 2017. Validity of radiocarbon ages of Siberian yedoma. GeoResJ. 13, 83–95.
- Vasil'chuk, Yu.K., Vasil'chuk, A.C., van der Plicht, J., Kutschera, W., Rank, D., 2001. Radiocarbon dating of the Late Pleistocene ice wedges in the Bison section in the lower reaches of the Kolyma River. Doklady Earth Sci. 379 (5), 589–593.
- Zharnikov, Z.Yu., Vizgalov, G.P., Knyazeva, E.V., Konovalenko, M.V., Myglan, V.S., 2013. Tree-ring chronology for Stadhinsky Ostrog. Ros. Arkheologiya, No. 6, 122–128.
- URL: <https://nucleus.iaea.org/wiser/index.aspx> [Partner: Northeast Science Station, Cherskij]. (submittal date: 24.05.2018).

Received September 21, 2017